DOI: 10.1021/ic9007558

Inorganic Chemistry
Article

^{129}I Mössbauer Spectroscopic Study of a Metallic MMX Chain System

Atsushi Kobayashi,*[,†,∥] Shinji Kitao,[‡] Makoto Seto,[‡] Ryuichi Ikeda,[†] and Hiroshi Kitagawa*[,†,§,⊥]

[†]*Department of Chemistry, Faculty of Science, Kyushu University, Hakozaki 6-10-1, Higashi-ku, Fukuoka 812-8581, Japan,* [‡]*Research Reactor Institute, Kyoto University, Kumatori, Sennan, Osaka 590-0494, Japan, and* [§]*JST-CREST, Sanbancho 5, Chiyoda-ku, Tokyo 102-0075, Japan.* [∥]*Present address: Division of Chemistry, Faculty of Science, Hokkaido University, North-10, West-8, Kita-ku, Sapporo 060-0810, Japan.* [⊥]*Present address: Department of Chemistry, Graduate School of Science, Kyoto University, Kitashirakawa Oiwakecho, Sakyo-ku, Kyoto 606-8502, Japan*

Received April 20, 2009

One-dimensional iodide-bridged mixed-valence binuclear platinum complexes (the so-called "MMX chains") and their Pt(III) dimer precursors were investigated with ^{129}I Mössbauer spectroscopy. Spectra consisting of two sets of octuplets were observed at low temperatures for a neutral MMX chain complex, $Pt_2(dtp)_4I$ ($dtp = C_2H_5CS_2^-$), with various charge-ordering states at the Pt dimers, indicating that the charge-ordering state is in an alternate-charge-polarization phase (ACP: $\cdots[Pt^{2+}-Pt^{3+}]-I^{0.4-}-[Pt^{3+}-Pt^{2+}]\cdots I^{0.3-}\cdots$), which is consistent with a previous low-temperature X-ray diffraction study. The estimated valence states of the bridging iodines of $[(C_2H_5)_2NH_2]_4[Pt_2(pop)_4I]$ ($pop = H_2P_2O_5^{2-}$), with a charge-polarization phase (CP: $\cdots[Pt^{2+}-Pt^{3+}]-I^{0.4-}\cdots[Pt^{2+}-Pt^{3+}]-I^{0.4-}\cdots$), and $[H_3N(CH_2)_6NH_3]_2[Pt_2(pop)_4I]$, with a charge-density-wave phase (CDW: $\cdots[Pt^{2+}-Pt^{2+}]\cdots I^{0.3-}-[Pt^{3+}-Pt^{3+}]-I^{0.3-}\cdots$), suggest that the covalent bond interaction is dominant in the CDW phase, whereas the Coulomb interaction is dominant in the CP phase. The estimated absolute quadrupole coupling constant (QCC) values for negatively charged MMX chain complexes with pop ligands are larger than those for neutral MMX chain complexes with $CH_3CS_2^-$ (dta) ligands, implying that the Madelung potential formed by the more-negative pop ligands and countercations effectively contributes to the physical properties of the pop system. The three Pt(III) dimer complexes $Pt_2(dta)_4I_2$, $Pt_2(dtp)_4I_2$, and $K_4[Pt_2(pop)_4I_2]$ showed almost the same isomer shifts, indicating that the valence state of the iodide ion ($I^{0.5-}$) depends negligibly on the terminal ligand. The QCC value observed for $K_4[Pt_2(pop)_4I_2]$ was larger than those for $Pt_2(dta)_4I_2$ and $Pt_2(dtp)_4I_2$, originating from the anisotropic arrangement of the iodide anions, which form layers lying on the *ab* plane in the crystal.

Introduction

One-dimensional (1-D) halogen-bridged mixed-valence binuclear metal complexes, the so-called "MMX chains", are one of the most attractive materials in 1-D electronic systems because of their characteristic electronic states and unique physical properties, such as their metallic conductivity and pressure- or light-induced phase transitions, spin-Peierls transitions, and so on.[1,2] The degrees of freedom of the charge polarization in the metal dimer units play an important role in the physical properties of MMX chain systems. Several charge-ordering states have been observed in the MMX chain and are listed as follows:

(1) Averaged valence (AV) state: $-[M^{2.5+}-M^{2.5+}]-X-[M^{2.5+}-M^{2.5+}]-X-$

(2) Charge-polarization (CP) state: $\cdots[M^{2+}-M^{3+}]-X\cdots[M^{2+}-M^{3+}]-X\cdots$

(3) Charge-density-wave (CDW) state: $\cdots[M^{2+}-M^{2+}]\cdots X-[M^{3+}-M^{3+}]-X\cdots$

(4) Alternate-charge-polarization (ACP) state: $\cdots[M^{2+}-M^{3+}]-X_a-[M^{3+}-M^{2+}]\cdots X_b\cdots$

So far, two types of MMX chain systems have been reported, classified by their terminal ligands. One is the pop system, represented as $A_4[Pt_2(pop)_4X]\cdot nH_2O$ ($A = Li^+$, Na^+, K^+, NH_4^+, etc.; pop = $H_2P_2O_5^{2-}$; $X = Cl^-$, Br^-, I^-), which consists of anionic MMX chains and countercations,

*To whom correspondence should be addressed. Tel.: +81-11-706-3818 (A.K.), +81-75-753-4035 (H.K.). Fax: +81-11-706-3447 (A.K.), +81-75-753-4035 (H.K.). E-mail: akoba@sci.hokudai.ac.jp (A.K.), kitagawa@kuchem.kyoto-u.ac.jp (H.K.).

(1) (a) Matsuzaki, H.; Matsuoka, T.; Kishida, H.; Takizawa, K.; Miyasaka, H.; Sugiura, K.; Yamashita, M.; Okamoto, H. *Phys. Rev. Lett.* **2003**, *90*, 046401. (b) Matsuzaki, H.; Kishida, H.; Okamoto, H.; Takizawa, K.; Matsunaga, S.; Takaishi, S.; Miyasaka, H.; Sugiura, K.; Yamashita, M. *Angew. Chem., Int. Ed.* **2005**, *44*, 3240–3243.

(2) (a) Kitagawa, H.; Onodera, N.; Sonoyama, T.; Yamamoto, M.; Fukawa, T.; Mitani, T.; Seto, M.; Maeda, Y. *J. Am. Chem. Soc.* **1999**, *121*, 10068–10080. (b) Mitsumi, M.; Murase, T.; Kishida, H.; Yoshinari, T.; Ozawa, Y.; Toriumi, K.; Sonoyama, T.; Kitagawa, H.; Mitani, T. *J. Am. Chem. Soc.* **2001**, *123*, 11179–11192. (c) Yamashita, M; Takaishi, S.; Kobayashi, A.; Kitagawa, H.; Matsuzaki, M.; Okamoto, H. *Coord. Chem. Rev.* **2005**, *250*, 2335–2346. (d) Wakabayashi, Y.; Kobayashi, A.; Sawa, H.; Ohsumi, H.; Ikeda, N.; Kitagawa, H. *J. Am. Chem. Soc.* **2006**, *128*, 6676–6682. (e) Otsubo, K.; Kobayashi, A.; Kitagawa, H.; Hedo, M.; Uwatoko, Y.; Sagayama, H.; Wakabayashi, Y.; Sawa, H. *J. Am. Chem. Soc.* **2006**, *128*, 8140–8141. (f) Saito, K.; Ikeuchi, S.; Nakazawa, Y.; Sato, A.; Mitsumi, M.; Yamashita, T.; Toriumi, K.; Sorai, M. *J. Phys. Chem. B* **2005**, *109*, 2956–2961. (g) Kobayashi, A.; Tokunaga, A.; Ikeda, R.; Sagayama, H.; Wakabayashi, Y.; Sawa, H.; Hedo, M.; Uwatoko, Y.; Kitagawa, H. *Eur. J. Inorg. Chem.* **2006**, 3567–3570.

Published on Web 07/16/2009

as shown in Figure 1a.[1,3] The other is the dta system, represented as $M_2(RCS_2)_4I$ (M = Pt, Ni; R = alkyl group), which consists of neutral MMX chains without counterions, as shown in Figure 1b.[2] Extensive work on both the pop and dta systems has revealed that the pop system exhibits semiconducting or insulating behavior whereas the dta system is highly conductive, and some platinum complexes exhibit metallic conduction and metal−insulator transitions.[1−4] The CP or CDW state of the pop system is the ground state, and some types undergo photoinduced or pressure-induced phase transitions between the CP and CDW phases. In contrast, in the dta system, the AV state is often observed in the metallic phase. At low temperatures, a metal−insulator transition occurs because of the strong electron−lattice interactions.[2] The ground state of the dta system is considered to be in the ACP state.[4e−g] These data clearly indicate that the electronic states in the dta and pop systems differ markedly, although their Pt dimer units are in the isoelectronic d^7−d^8 configuration. The origin of these differences in their electronic states is still under discussion. Except for some theoretical studies,[5,6] there have been few systematic studies of the two MMX chain systems. To gain insight into the origin of the differences between the dta and pop systems, some *quantitative* measurements must be made to investigate the electronic states of the MMX chain complexes. Mössbauer spectroscopy has been widely used to investigate the valence states of measurable atoms (such as ^{57}Fe, ^{119}Sn, ^{129}I, and ^{197}Au).[7] The Mössbauer parameters, isomer shift (IS) and the quadrupole coupling constant (QCC), allow us to discuss the electronic states of measured atoms quantitatively. Therefore, we have used ^{129}I Mössbauer spectroscopy to probe the differences between the electronic states of the two MMX chain systems. We also measured as controls the spectra of Pt(III) dimer complexes, which are the precursors of MMX chain complexes.

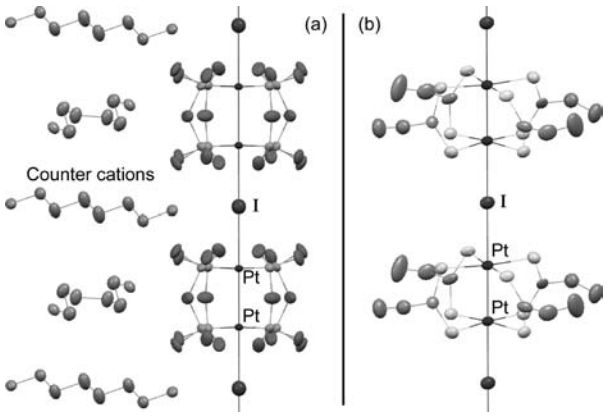

Figure 1. Crystal structures of (a) $[NH_3(CH_2)_6NH_3]_2[Pt_2(pop)_4I]$ and (b) $Pt_2(dtp)_4I$.

In this paper, we report the ^{129}I Mössbauer spectra of these two types of MMX chain systems, and we discuss the electronic states of the iodide-bridged MMX chain complexes quantitatively.

Experimental Section

Synthesis. The starting materials, tetrakis(dithioacetato)diplatinum(II), $Pt_2(dta)_4$ (dta = $CH_3CS_2^-$);[8] tetrakis(dithiopropionate)diplatinum(II), $Pt_2(dtp)_4$ (dtp = $CH_3CH_2CS_2^-$);[9] and potassium tetrakis(pyrophosphito)diplatinate(II), $K_4[Pt_2(pop)_4]$,[10] were prepared according to the published procedures.

Sample Preparation for ^{129}I Mössbauer Spectroscopy. The samples for iodine Mössbauer spectroscopy were synthesized using the radioisotope ^{129}I at the Kyoto University Reactor (KUR) with the following chemical reactions.

For $Pt_2(dta)_4I_2$ (**1**), $Pt_2(dtp)_4I_2$ (**2**), and $Pt_2(dtp)_4I$ (**3**):

$$2Na^{129}I + Na_2SO_3 + 2H_2O_2 + H_2SO_4 \rightarrow 2Na_2SO_4 + 3H_2O + {}^{129}I_2 \quad \text{(I)}$$

$$Pt_2(dta)_4 + {}^{129}I_2 \rightarrow Pt_2(dta)_4{}^{129}I_2\ (\mathbf{1}) \quad \text{(II)}$$

(3) (a) Che, C. M.; Schaefer, W. P.; Grey, H. B.; Dickson, M. K.; Stein, P. B.; Roundhill, D. M. *J. Am. Chem. Soc.* **1982**, *104*, 4253–4255. (b) Stein, P.; Dickson, M. K.; Roundhill, D. M. *J. Am. Chem. Soc.* **1983**, *105*, 3489–3494. (c) Kurmoo, M.; Clark, R. J. H. *Inorg. Chem.* **1985**, *24*, 4420–4425. (d) Clark, R. J. H.; Kurmoo, M. *J. Chem. Soc., Dalton Trans.* **1985**, 579–586. (e) Che, C. M.; Herbstein, F. H.; Schaefer, W. P.; Marsh, R. E.; Gray, H. B. *J. Am. Chem. Soc.* **1983**, *105*, 4604–4607. (f) Swanson, B. I.; Stroud, M. A.; Conradson, S. D.; Zietlow, M. H. *Solid State Commun.* **1988**, *65*, 1405–1409. (g) Butler, L. G.; Zietlow, M. H.; Che, C. M.; Schaefer, W. P.; Sridhar, S.; Grunthaner, P. J.; Swanson, B. I.; Clark, R. J. H.; Gray, H. B. *J. Am. Chem. Soc.* **1988**, *110*, 1155–1162. (h) Kimura, N.; Ohki, H.; Ikeda, R.; Yamashita, M. *Chem. Phys. Lett.* **1994**, *220*, 40. (i) Yamashita, M.; Miya, S.; Kawashima, T.; Manabe, T.; Sonoyama, T.; Kitagawa, H.; Mitani, T.; Okamoto, H.; Ikeda, R. *J. Am. Chem. Soc.* **1999**, *121*, 2321–2322. (j) Yamashita, M.; Takizawa, K.; Matsunaga, S.; Kawakami, D.; Iguchi, H.; Takaishi, S.; Kajiwara, T.; Miyasaka, H.; Sugiura, K.; Matsuzaki, H.; Okamoto, H.; Wakabayashi, Y.; Sawa, H. *Bull. Chem. Soc. Jpn.* **2006**, *79*, 1404–1406. (k) Matsunaga, S.; Takizaki, K.; Kawakami, D.; Iguchi, H.; Takaishi, S.; Kajiwara, T.; Miyasaka, H.; Yamashita, M.; Matsuzaki, H.; Okamoto, H. *Eur. J. Inorg. Chem.* **2008**, 3269–3273. (l) Iguchi, H.; Takaishi, S.; Kajiwara, T.; Miyasaka, H.; Yamashita, M.; Matsuzaki, H.; Okamoto, H. *J. Am. Chem. Soc.* **2008**, *130*, 17668–17669. (m) Iguchi, H.; Takaishi, M.; Kajiwara, T.; Miyasaka, H.; Yamashita, M.; Matsuzaki, H.; Okamoto, H. *J. Inorg. Organomet. Polym.* **2009**, *19*, 85–90.

(4) (a) Bellitto, C.; Flamini, A.; Gastaldi, L.; Scaramuzza, L. *Inorg. Chem.* **1983**, *22*, 444–449. (b) Bellitto, C.; Dessy, G.; Fares, V. *Inorg. Chem.* **1985**, *24*, 2815–2820. (c) Kitagawa, H.; Onodera, N.; Ann, J. S.; Mitani, T.; Toriumi, K.; Yamashita, M. *Mol. Cryst. Liq. Cryst.* **1996**, *285*, 311. (d) Kitagawa, H.; Onodera, N.; Mitani, T.; Toriumi, K.; Yamashita, M. *Synth. Met.* **1997**, *86*, 1931–1932. (e) Mitsumi, M.; Kitamura, K.; Morinaga, A.; Ozawa, Y.; Kobayashi, M.; Toriumi, K.; Iso, Y.; Kitagawa, H.; Mitani, T. *Angew. Chem., Int. Ed.* **2002**, *41*, 2767–2771. (f) Kitagawa, H.; Sonoyama, T.; Mitani, T.; Seto, M.; Maeda, Y. *Synth. Met.* **1999**, *103*, 2159. (g) Kitagawa, H.; Mitani, T. *Coord. Chem. Rev.* **1999**, *190−192*, 1169–1184. (h) Makiura, R.; Kitagawa, H.; Ikeda, R. *Mol. Cryst. Liq. Cryst.* **2002**, *379*, 309–314. (i) Mitsumi, M.; Umebayashi, S.; Ozawa, Y.; Toriumi, K.; Kitagawa, H.; Mitani, T. *Chem. Lett.* **2002**, 258–259. (j) Kobayashi, A.; Kitagawa, H.; Ikeda, R.; Kitao, S.; Seto, M.; Mitsumi, M.; Toriumi, K. *Synth. Met.* **2003**, *135−136*, 405. (k) Kobayashi, A.; Kojima, T.; Ikeda, R.; Kitagawa, H. *Inorg. Chem.* **2006**, *45*, 322–327. (l) Kobayashi, A.; Kitagawa, H. *J. Am. Chem. Soc.* **2006**, *128*, 12066–12067.

(5) (a) Yamamoto, S. *J. Phys. Chem. Solids* **2002**, *63*, 1489–1493. (b) Yamamoto, S. *J. Phys. Soc. Jpn.* **2001**, *70*, 1198–1201. (c) Yonemitsu, K.; Miyashita, N. *Phys. Rev. B* **2003**, *68*, 075113. (d) Yamamoto, S.; Ichioka, M. *J. Phys. Soc. Jpn.* **2002**, *71*, 189–196. (e) Ohara, J.; Yamamoto, S. *Phys. Rev. B* **2004**, *70*, 115112. (f) Ohara, J.; Yamamoto, S. *J. Phys. Soc. Jpn.* **2005**, *74*, 250–253. (g) Ohara, J.; Yamamoto, S. *J. Phys. Chem. Solids* **2005**, *66*, 1571–1574.

(6) (a) Kuwabara, M.; Yonemitsu, K. *J. Mater. Chem.* **2001**, *11*, 2163–2175. (b) Kuwabara, M.; Yonemitsu, K. *Physica B* **2000**, *284−288*, 1545–1546.

(7) (a) Parish, R. V. Mössbauer Spectroscopy Applied to Inorganic Chemistry. In *Mössbauer Spectroscopy with Iodine Isotopes*; Long, G. J., Ed.; Plenum: New York, 1984; Vol. *2*, p 391 and references therein. (b) Ruby, S. L.; Shenoy, G. K. In *Mössbauer Isomer Shifts*; Hendy, G. K., Wagner, F. E., Eds; North-Holland: Amsterdam, 1978; Chapter 9b.

(8) Bellitto, C.; Flamini, A.; Piovesana, O.; Zanazzi, P. F. *Inorg. Chem.* **1980**, *19*, 3632.

(9) Mitsumi, M.; Yoshinari, T.; Ozawa, Y.; Toriumi, K. *Mol. Cryst. Liq. Cryst.* **2000**, *342*, 127.

(10) Che, C. M.; Butler, L. G.; Grunthaner, P. J.; Gray, H. B. *Inorg. Chem.* **1985**, *24*, 4662–4665.

Table 1. Mössbauer Parameters for MMX Chain Complexes and Their Precursors

complex	terminal ligand	T (K)	IS[a] (mm s^{-1})	QCC (MHz)	h_p[b]	U_p	ρ[c]	area
1	$CH_3CS_2^-$	16	3.66(7)	−1172(35)	0.47(4)	0.51(2)	−0.53(4)	
2	$C_2H_5CS_2^-$	16	3.71(7)	−1177(35)	0.51(4)	0.51(2)	−0.49(4)	
3-I$_a$	$C_2H_5CS_2^-$	11	3.94(8)	−1213(36)	0.59(5)	0.53(2)	−0.41(5)	0.85(1)
3-I$_b$		11	3.99(8)	− 1432(43)	0.69(5)	0.62(2)	− 0.31(5)	1.00
3-I$_a$	$C_2H_5CS_2^-$	80	3.80(7)	−1238(37)	0.56(4)	0.54(2)	−0.44(4)	0.79(2)
3-I$_b$		80	3.95(8)	− 1413(42)	0.67(5)	0.62(2)	− 0.33(5)	1.00
4	$H_2P_2O_5^{2-}$	16	3.64(7)	−1530(46)	0.46(4)	0.67(2)	−0.54(4)	
5	$H_2P_2O_5^{2-}$	15	3.80(7)	−1567(47)	0.57(4)	0.68(2)	−0.43(4)	
6	$H_2P_2O_5^{2-}$	15	3.96(8)	−1680(50)	0.67(5)	0.73(2)	−0.33(5)	

[a] Referenced to Mg_3TeO_6. [b] Calculated from eq 2 with h_s set to zero. [c] Calculated with the equation $\rho = h_p - 1$.

$$Pt_2(dtp)_4 + {}^{129}I_2 \rightarrow Pt_2(dtp)_4{}^{129}I_2\ (\mathbf{2}) \qquad (III)$$

$$Pt_2(dtp)_4 + Pt_2(dtp)_4{}^{129}I_2 \rightarrow 2Pt_2(dtp)_4{}^{129}I\ (\mathbf{3}) \qquad (IV)$$

Reaction I is the extraction process for $^{129}I_2$ from aqueous solution. The sample preparation processes II, III, and IV were performed according to the procedures published previously.[2b]

For $K_4[Pt_2(pop)_4I_2]$ (**4**), $[(C_2H_5)_2NH_2]_4[Pt_2(pop)_4I]$ (**5**), and $[NH_3(CH_2)_6NH_3]_2[Pt_2(pop)_4I]$ (**6**):

$$2Na^{129}I + Pb(CH_3COO)_2 \rightarrow 2CH_3COONa + Pb^{129}I_2 \qquad (V)$$

$$Pb^{129}I_2 + Na_2CO_3 \rightarrow 2Na^{129}I + PbCO_3 \qquad (VI)$$

$$Na^{129}I + {}^{127}I_2 \rightarrow Na^{129}I^{127}I_2 \qquad (VII)$$

$$Na^{129}I^{127}I_2 + K_4[Pt_2(pop)_4] \rightarrow NaI + K_4[Pt_2(pop)_4I_2]\ (\mathbf{4}) \qquad (VIII)$$

$$K_4[Pt_2(pop)_4I_2] + K_4[Pt_2(pop)_4] + ex.((C_2H_5)_2NH_2)_2SO_4 \rightarrow [(C_2H_5)_2NH_2]_4[Pt_2(pop)_4I]\ (\mathbf{5}) \qquad (IX)$$

$$K_4[Pt_2(pop)_4I_2] + K_4[Pt2(pop)_4] + ex.(H_3N(CH_2)_6NH_3)SO_4 \rightarrow [NH_3(CH_2)_6NH_3]_2[Pt_2(pop)_4I]\ (\mathbf{6}) \qquad (X)$$

Reactions V, VI, and VII are purification processes for $^{129}I^-$. The sample preparation processes VIII, IX, and X were performed according to the published procedures.[3]

^{129}I Mössbauer Spectroscopy. A ^{129m}Te source was obtained by the neutron irradiation of enriched $Mg_3{}^{128}TeO_6$ in the nuclear reaction ^{128}Te[n,γ]^{129m}Te at KUR. The half-life of ^{129m}Te is 33 days. Mössbauer spectroscopic measurement of a 27.7 keV γ-ray transition in ^{129}I was carried out while both the source and the absorber were cooled, using a constant-acceleration spectrometer with a NaI(Tl) scintillation counter and a Daikin CryoKelvin closed-cycle refrigerator system using helium gas as the working medium.

Analysis of ^{129}I Mössbauer Spectra. The observed spectra were analyzed with a computer program that included folding and least-squares fitting with Lorentzian lines. The half-life of the excited state is rather long (16.8 ns), producing well-resolved spectra with small natural line widths. The nuclear spins of the excited and ground states are 5/2 and 7/2, respectively. Therefore, the quadrupole-split spectra consisted of a minimum of eight lines. For all six measured complexes, IS, QCC, the number of p holes (h_p), the p-electron imbalance (U_p), the charge on the iodine (ρ), and the relative integral intensity (area) are given in Table 1. The relationship between the Mössbauer parameters and the valence shell configuration of the iodine atom has been discussed many times.[7] IS is given by

$$IS = C\Delta\langle R^2\rangle\Delta\rho(0) \qquad (1)$$

where C is a constant containing the nuclear parameters (>0), $\Delta\langle R^2\rangle$ is the change in the square of the nuclear radius between the excited and ground states, which has been estimated to be $+19.5 \times 10^3$ fm^2 for ^{129}I, and $\Delta\rho(0)$ is the difference between the contact densities of the source and the absorber. Therefore, for ^{129}I, a positive IS indicates an increase in the electron density at the nucleus, $\rho(0)$. In the case of the iodide ion, which has a $5s^25p^6$ configuration, the IS value is given by the following empirical equation:[7]

$$IS = -9.2h_s + 1.5h_p - 0.54 \qquad (2)$$

where the IS values (mm s^{-1}) are referenced to ZnTe and h_s and h_p are the hole numbers of the s and p shells, respectively. Therefore, the oxidation state of the iodine atom can be estimated from this equation. The iodine atom has a larger IS value, in the order $I^- < I^0 < I^+$, because of the reduction in the occupation of the p orbitals in this order, because the valence and core s orbitals are screened from the nucleus. Therefore, the IS value reflects the number of both s and p electrons. When the s electron of iodine does not contribute to the Pt−I bond, we can assume that the h_s value is zero. Conversely, the QCC is a direct measure of the electric field gradient (EFG) at the iodine nucleus:[7]

$$QCC = e^2qQ \qquad (3)$$

where e is the charge on the proton ($e > 0$), Q is the nuclear quadrupole moment (negative for both the excited and ground states of ^{129}I), and EFG is often designated eq (principal [z] component of EFG). The concentration of the negative charge on the xy plane makes EFG positive (QCC is negative because eQ is negative for ^{129}I), and that on the z axis makes it negative (QCC is positive). Most of the iodide (I^-), iodine (I^0), and iodine cation (I^+) complexes have negative QCC values, because as the electronic configurations range from the closed-shell iodide ion, $5s^25p^6$, to the neutral iodine atom I, $5s^25p^5$, to the iodine cation (I^+), $5s^25p^4$, the electron density is steadily lost from the $5p_z$ orbital along the series. Therefore, an IS−QCC linear correlation is well-known in this series. The following relationship is also well-known for nuclear quadrupole resonance data:[7]

$$U_p = h_z - (h_x + h_y)/2 \qquad (4)$$

$$U_p = -e^2qQ^{127}h^{-1}/2293\ \text{MHz} \qquad (5)$$

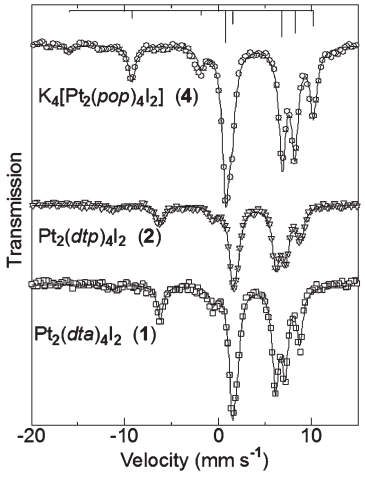

Figure 2. ^{129}I Mössbauer spectra of the MMX chain precursors **1**, **2**, and **4**.

where U_p is the difference between the populations of iodine $5p_z$ orbitals and the $5p_x$ and $5p_y$ orbitals, and is sometimes referred to as the p-electron imbalance, and h_n ($n = x, y, z$) is the hole number of the p_n orbitals. The QCC value purely reflects the number of p electrons. The s electron has no effect on the QCC value because the electron density is spherically symmetrical. When an I atom has no π-bonding character, the assumption that $h_x = h_y = 0$ is valid because the p_x and p_y electrons only contribute to the π bond.

Results and Discussion

^{129}I Mössbauer Spectra of the MMX Chain Precursors. The ^{129}I Mössbauer spectra for the precursors of the MMX chain complexes $Pt_2(dta)_4I_2$ (**1**), $Pt_2(dtp)_4I_2$ (**2**), and $K_4[Pt_2(pop)_4I_2]$ (**4**) at 16 K are shown in Figure 2. The Mössbauer parameters obtained are summarized in Table 1. The three Pt(III) dimer complexes have the same isoelectronic configuration (d^7–d^7) and lantern-type $Pt^{3+}{}_2(L)^4I_2$ molecular structure.[4a,2b,11] The differences among them are the terminal ligands L and their charges. Complexes **1** and **2** are composed of neutral molecules with $CH_3CS_2^-$ and $C_2H_5CS_2^-$ ligands, respectively, whereas complex **4** is composed of K^+ and anionic molecules $[Pt_2(pop)_4I_2]^{4-}$ with a more negatively charged $H_2P_2O_5^{2-}$ ligand.

The best fit for each spectrum was obtained with one octuplet, indicating that only one chemically independent iodide site exists in each complex, which corresponds to each crystal structure.[2b,11] The spectra of **1** and **2** were almost the same, indicating that the dta and dtp ligands have the same σ-donation effect via Pt ions on the valence state of iodine. In contrast, the quadrupole splitting in **4** was significantly larger than that in **1** or **2**. Nevertheless, the values for IS for these three complexes are very close (3.62–3.71 mm s^{-1}).

The valence state of iodine can be estimated from both the IS and QCC values. If the s and p_π orbitals of iodine do not contribute to the Pt–I bond, the number of p holes (h_p) estimated from IS and the p-electron imbalance (U_p) estimated from QCC should agree (see the section on the analysis of the ^{129}I Mössbauer spectrum in the Experimental Section).[7] The estimated h_p and U_p values for complexes **1** and **2** were almost the same (ca. 0.5), indicating that these assumptions are valid. However, as described above, the QCC value for **4** was larger by ca. 400 MHz than that for **1** or **2**, despite their similar IS values. The larger QCC value observed for **4** is probably attributable to the alternate stacking of the $Pt_2(pop)_4I_2^{4-}$ units and the potassium cations along the *c* axis.[11] As shown in Figure 3, the iodide anions lie on the same *ab* planes, whereas they are located between the Pt and K cations along the *c* axis. This arrangement of cations and anions around the iodide ions (i.e., negative charges on the *ab* plane and positive charges along the *c* axis) apparently increases the EFG at the iodide nucleus. As a result, a larger QCC was observed for **4**, even though the electron density at the nucleus of iodine and the EFG derived from the p-electron density imbalance in **4** are almost the same as those in **1** and **2**. The crystal structure of neutral **2** does not show such regular stacking of cations and anions.[2b] From their IS values, the oxidation states (ρ) of the iodide ions were estimated to be −0.5. The larger QCC value of **4** is attributed to the Coulomb potential from the counter cations and the more-negatively charged pop ligand.

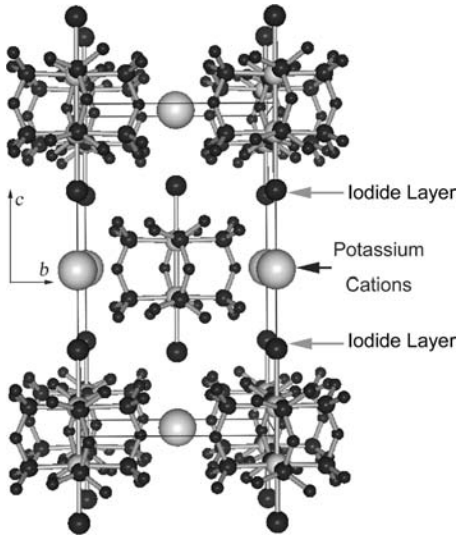

Figure 3. Crystal structure of complex **4** (ref 11). Cations (Pt and K) and anions (I and pop ligand) are shown in gray and black, respectively.

^{129}I Mössbauer Spectra of MMX Chain Complexes. The ^{129}I Mössbauer spectra of the MMX chain complexes $Pt_2(dtp)_4I$ (**3**), $[(C_2H_5)_2NH_2]_4[Pt_2(pop)_4I]$ (**5**), and $[NH_3(CH_2)_6NH_3]_2[Pt_2(pop)_4I]$ (**6**) are shown in Figure 4. The Mössbauer parameters obtained for them are summarized in Table 1. In previous works,[1a,4e] MMX chain complexes **3**, **5**, and **6** were found to have different 1-D charge orderings in their ground states: an ACP state for **3** (ACP: $\cdots[Pt^{2+}-Pt^{3+}]-I-[Pt^{3+}-Pt^{2+}]\cdots I\cdots$), a CP state for **5** (CP: $\cdots[Pt^{2+}-Pt^{3+}]-I\cdots[Pt^{2+}-Pt^{3+}]-I\cdots$), and a CDW state for **6** (CDW: $\cdots[Pt^{2+}-Pt^{2+}]\cdots I-[Pt^{3+}-Pt^{3+}]-I\cdots$). It is clear that the observed spectra for the MMX chain complexes are quite different. The spectrum of **3** consists of two sets of octuplets, whereas the spectra of **5** and **6** consist of one octuplet. The IS and QCC values for **6** are larger by about

(11) Alexander, K. A.; Bryan, S. A.; Fronczek, F. R.; Fultz, W. C.; Rheingold, A. L.; Roundhill, D. M.; Stein, P.; Watkins, S. F. *Inorg. Chem.* **1985**, *24*, 2803–2808.

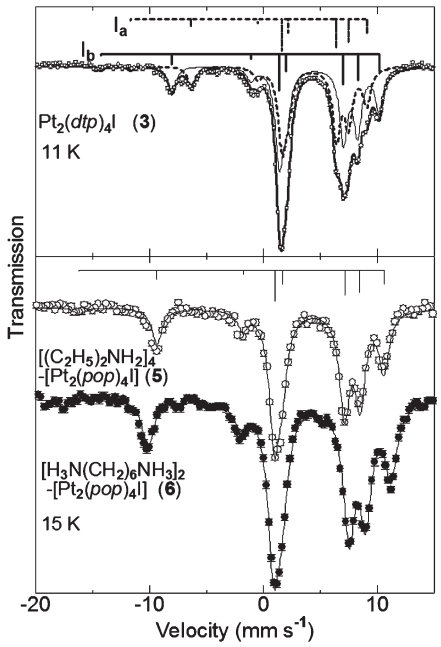

Figure 4. ^{129}I Mössbauer spectra of MMX chain complexes **3** (at 11 K), **5**, and **6** (at 15 K).

0.2 mm s^{-1} and 120 MHz, respectively, than those for **5**. These results should reflect the characters of the ACP, CP, and CDW states.

According to the X-ray crystal structural analysis by Mitsumi et al.,[4e] complex **3** is in the ACP phase at 48 K, where two chemically independent iodine sites are situated between the Pt^{3+} sites and between the Pt^{2+} sites. Of the four kinds of charge-ordering phases, only the ACP phase has two chemically independent iodine sites. Therefore, the observed spectrum for **3** is consistent with the X-ray crystal structure study. These two chemically independent iodine sites are denoted I_a and I_b in Figure 4 and Table 1. Because the QCC value of the I_a site in **3** is closer to that in the Pt(III) dimer complex **1** or **2**, the two sites I_a and I_b can be assigned as follows: $\cdots[Pt^{2+}-Pt^{3+}]-I_a-[Pt^{3+}-Pt^{2+}]\cdots I_b\cdots[Pt^{2+}-Pt^{3+}]-I_a-[Pt^{3+}-Pt^{2+}]\cdots I_b\cdots$ This assignment is consistent with our previous work.[2a]

Complex **3** exhibits high electrical conductivity (~5 S cm^{-1}) and a metal−insulator transition at 205 K. Its electronic state changes with the temperature: the AV state with a CDW fluctuation above 205 K, the CP state at 160−205 K, and the ACP state below 160 K.[2a−e,4e] Especially below 110 K, the 2-fold diffuse scatterings at $k = n + 0.5$ (k corresponds to the 1-D chain axis; n is an integer) gradually varied to superlattice Bragg spots,[2b] which indicates the gradual distortion of the ACP-type $\cdots[Pt^{2+}-Pt^{3+}]-I_a-[Pt^{3+}-Pt^{2+}]\cdots I_b\cdots$ with decreasing temperature and the 3-D ordering of the ACP state at 48 K. This distortion is similar to a spin-Peierls-like distortion. Comparing the relative integral intensities (areas) of I_a and I_b at 11 K with those at 80 K, the area of I_a (0.85(1)) at 11 K was larger than that (0.79(2)) at 80 K. It is well-known that the area intensity relates to the recoil-free fraction at the nucleus. Roughly speaking, the more tightly an atom is bound in a crystal, the larger its recoil-free fraction becomes.[12] The fact that the relative intensity of the I_a site increased with decreasing temperature is consistent with the procession of the ACP-type distortion, because the I_a site becomes more rigid at lower temperatures because of this distortion. Therefore, the increase in the relative intensity of the I_a site with ACP-type distortion also supports our assignment discussed above. From the QCC values of **3**, the chain structure and oxidation states of I are considered to be as follows: $\cdots[Pt^{2+}-Pt^{3+}]-I_a^{0.41-}-[Pt^{3+}-Pt^{2+}]\cdots I_b^{0.31-}\cdots$ The valence state of Pt expressed as a $-Pt^{2+}-Pt^{3+}-$ represents a formal oxidation number. In the isoelectronic complex $Pt_2(dta)_4I$ (**7**), almost the same results for the Mössbauer parameters were observed. The fact that the more-negative $I_a^{0.41-}$ is located between the more-positive Pt^{3+}'s suggests that the Coulomb interaction plays an important role in the ACP electronic state of the dta system.

It is noteworthy that the intensity ratio of the two components should be 1.0, because of the I_a/I_b compositional ratio in stoichiometric $Pt_2(dtp)_4I$. In the ACP phase, we assume that the recoil-free fraction of I_a between the Pt^{3+} sites is larger than that of I_b between the Pt^{2+} sites, because the $Pt^{3+}-I_a$ distance is shorter than the $Pt^{2+}\cdots I_b$ distance. The results were the reverse at both 11 and 80 K, which might be attributable to the competition between the ACP- and CDW-type distortions or the incomplete 3-D ordering of the ACP phase. It is well-known that Peierls- or spin-Peierls-type lattice distortions cannot be ordered three dimensionally, even at 0 K, in a pure 1-D electronic system. In fact, complex **3** has a nearest-neighbor interchain distance about 1.4 Å longer than that of **7**, which has a shorter alkyl-chain ligand. It is possible that the ACP-type lattice distortion was still not completely ordered in three dimensions at 11 K.

Conversely, the observed spectra for the complexes of the pop system, **5** and **6**, consisted of one octuplet, indicating that only one iodine site exists in these complexes. The obtained spectra for **5** and **6** around 50 K were the same as the spectra at 16 K. Above 80 K, owing to a very low recoil-free fraction, the spectra became very weak and finally meaningless. On the basis of the magnetic susceptibility and Raman spectra for these complexes reported by Matsuzaki et al.,[1a] the charge-ordering states of complexes **5** and **6** are considered to be CP and CDW, respectively. Because these phases contain only one iodine site, located between the Pt^{3+} and Pt^{2+} ions, the observed temperature-independent spectra consisting of one octuplet are consistent with previous reports. It is noteworthy that the valence states of iodine in **5** and **6** are significantly different. The oxidation state ρ of iodine in the CP complex **5** is estimated from the IS values to be −0.43(4), which is lower than that for the CDW complex **6** (−0.33(5)). X-ray structural studies of complexes **5** and **6** revealed that the Pt−I bond distance is 2.718 Å in **5**,[1a] which is slightly shorter than that in the Pt(III) dimer complex **4** (2.746 Å),[11] whereas that in **6** is markedly longer by about 0.2 Å (2.922 Å).[1a] From the viewpoint of ligand field theory, the short Pt−I bond should destabilize the $5d_{z^2}$ orbital of Pt^{3+} and stabilize the $5p_z$ orbital of I^-. In contrast, the overlap integral between these orbitals

(12) Viegers, T. P. A.; Trooster, J. M.; Brouten, P.; Rit, T. P. *J. Chem. Soc., Dalton Trans.* **1977**, 2074.

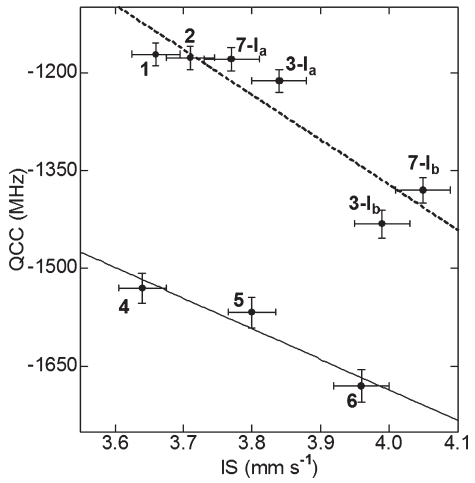

Figure 5. IS−QCC correlation diagram for complexes **1**−**6** and $Pt_2(dta)_4I$ (**7**).[2a] Solid and dashed lines represent guides for the pop and dta systems, respectively.

should be larger for the shorter Pt−I bond. Thus, if the Coulomb interaction is more dominant than the covalent bond interaction, the more-reduced iodine (i.e., the iodide ion) connects to the Pt^{3+} ion. The fact that iodine is more reduced in the CP state of **5** ($I^{0.43-}$) than in the CDW state of **6** ($I^{0.33-}$) suggests that the Coulomb interaction plays a more important role in the CP phase. In contrast, the covalent bond interaction is more dominant in the CDW phase.

Effect of the Terminal Ligand of the MMX Chain System. As described in the Introduction, all MMX chain complexes can be classified into two systems, the pop and dta systems, according to their terminal ligands. These two systems exhibit significantly different physical properties, although they have the same electronic configurations (d^7−d^8) in the Pt dimer unit. In this section, the difference in the electronic states of the dta and pop systems is discussed. Figure 5 shows an IS−QCC correlation diagram for complexes **1**−**6** and $Pt_2(dta)_4I$ (**7**), which is the first metallic MMX chain complex.[2a] It is well-known that a linear correlation exists between the IS and QCC values for the series of the iodide anion (I^-), iodine (I^0), and the iodine cation (I^+).[7] Iodide ions in the MMX chain systems were also found to follow this linear IS−QCC correlation. However, when analyzed in more detail, the dta and pop systems seem to follow different IS−QCC linear correlations (see the guides shown as dashed and solid lines in Figure 5). The IS values depend only on the coordination environment of iodine and depend negligibly on the terminal ligand. The IS values for the terminal iodine in the discrete Pt(III) dimer ($I-Pt^{3+}-Pt^{3+}-I$) are around 3.7 mm s^{-1}, and those for the bridging iodine in the MMX chain complexes are about 0.1−0.4 mm s^{-1} higher. Conversely, the QCC values seem to depend on the terminal ligands. The QCC values for the pop system (complexes **4**, **5**, and **6**) are markedly larger, by about 300 MHz, than those for the dta system (complexes **1**, **2**, **3**, and **7**). The QCC value reflects the electric field gradient at the iodine nucleus, which includes the contribution not only from the 5p electron imbalance but also from the charge on the ions surrounding the iodine. Although a few data points in the IS−QCC correlation diagram give conclusive information, the fact that larger absolute QCC values were observed for the pop system implies that the positive charge on the countercation and the more-negatively charged terminal ligand significantly affect the electronic state of the 1-D MMX chain. In other words, the differences in the electronic states of the highly conductive dta system and the insulating pop system originate from the difference in the Coulomb interaction in the 1-D chains, which are indirectly affected by the terminal ligands or counterions.

Conclusion

^{129}I Mössbauer spectroscopy was applied to two different kinds of MMX chain systems and Pt(III) dimers. The almost identical IS values for the dimers $Pt_2(dta)_4I_2$ (**1**), $Pt_2(dtp)_4I_2$ (**2**), and $K_4[Pt_2(pop)_4I_2]$ (**4**) indicate that the valence state of iodine ($I^{0.5-}$) does not depend on the terminal ligand. The QCC value for **4** was larger than those for **1** and **2**, which is attributed to the anisotropic arrangement of the iodide ions, which form a layer lying on the *ab* plane in the crystal. The Mössbauer spectra observed for the three MMX chain complexes $Pt_2(dtp)_4I$ (**3**), $[(C_2H_5)_2NH_2]_4[Pt_2(pop)_4I]$ (**5**), and $[H_3N(CH_2)_6NH_3]_2[Pt_2(pop)_4I]$ (**6**) reflect the characters of their charge-ordering phases: ACP (ACP: $\cdots[Pt^{2+}-Pt^{3+}]-I_a^{0.4-}-[Pt^{3+}-Pt^{2+}]\cdots I_b^{0.3-}\cdots$) for **3**; CP (CP: $\cdots[Pt^{2+}-Pt^{3+}]-I_a^{0.4-}\cdots[Pt^{2+}-Pt^{3+}]-I^{0.4-}\cdots$) for **5**; and CDW phase (CDW: $\cdots[Pt^{2+}-Pt^{2+}]-I^{0.3-}-[Pt^{3+}-Pt^{3+}]-I^{0.3-}\cdots$) for **6**. The Mössbauer parameters for **3**, especially the fact that the more-negative $I_a^{0.41-}$ is located between the more-positive Pt^{3+}'s, suggest that the Coulomb interaction plays an important role in the ACP electronic state of the dta system. Conversely, the oxidation states estimated for iodine in **5** ($I^{0.4-}$) and **6** ($I^{0.3-}$) suggest that the Coulomb interaction predominates in the CP phase and that the covalent bond interaction predominates in the CDW phase. The fact that larger absolute QCC values were observed for the pop system relative to those for the dta system, despite their similar IS values, implies that the Madelung potential given by the more-negative terminal pop ligand and the counter cations is responsible for the differences in the physical properties of the dta and pop systems.

Acknowledgment. This work was partly supported by Grant-in-Aid for Scientific Research for Priority Areas (Chemistry of Coordination Space) no. 16074212 and the Joint Project for Chemical Synthesis Core Research Institutions from the Ministry of Education, Culture, Sports, Science and Technology, Japan, and by Grants-in-Aid for Scientific Research (B) no. 14340215 and no. 16350033 from the Japan Society for the Promotion of Science, and by Kurata Memorial Hitachi Science.